

This is a repository copy of *Influence of bromine and iodine chemistry on annual, seasonal, diurnal, and background ozone : CMAQ simulations over the Northern Hemisphere*.

White Rose Research Online URL for this paper:
<https://eprints.whiterose.ac.uk/147482/>

Version: Accepted Version

Article:

Sarwar, Golam, Gantt, Brett, Foley, Kristen et al. (8 more authors) (2019) Influence of bromine and iodine chemistry on annual, seasonal, diurnal, and background ozone : CMAQ simulations over the Northern Hemisphere. *Atmospheric Environment*. pp. 395-404. ISSN 1352-2310

<https://doi.org/10.1016/j.atmosenv.2019.06.020>

Reuse

This article is distributed under the terms of the Creative Commons Attribution-NonCommercial-NoDerivs (CC BY-NC-ND) licence. This licence only allows you to download this work and share it with others as long as you credit the authors, but you can't change the article in any way or use it commercially. More information and the full terms of the licence here: <https://creativecommons.org/licenses/>

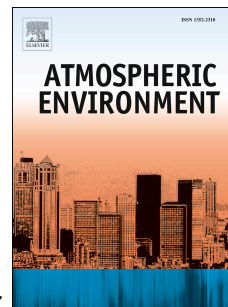
Takedown

If you consider content in White Rose Research Online to be in breach of UK law, please notify us by emailing eprints@whiterose.ac.uk including the URL of the record and the reason for the withdrawal request.

Accepted Manuscript

Influence of bromine and iodine chemistry on annual, seasonal, diurnal, and background ozone: CMAQ simulations over the Northern Hemisphere

Golam Sarwar, Brett Gantt, Kristen Foley, Kathleen Fahey, Tanya L. Spero, Daiwen Kang, Rohit Mathur, Hosein Foroutan, Jia Xing, Tomás Sherwen, Alfonso Saiz-Lopez



PII: S1352-2310(19)30411-X

DOI: <https://doi.org/10.1016/j.atmosenv.2019.06.020>

Reference: AEA 16782

To appear in: *Atmospheric Environment*

Received Date: 19 October 2018

Revised Date: 7 June 2019

Accepted Date: 8 June 2019

Please cite this article as: Sarwar, G., Gantt, B., Foley, K., Fahey, K., Spero, T.L., Kang, D., Mathur, R., Foroutan, H., Xing, J., Sherwen, Tomás., Saiz-Lopez, A., Influence of bromine and iodine chemistry on annual, seasonal, diurnal, and background ozone: CMAQ simulations over the Northern Hemisphere, *Atmospheric Environment* (2019), doi: <https://doi.org/10.1016/j.atmosenv.2019.06.020>.

This is a PDF file of an unedited manuscript that has been accepted for publication. As a service to our customers we are providing this early version of the manuscript. The manuscript will undergo copyediting, typesetting, and review of the resulting proof before it is published in its final form. Please note that during the production process errors may be discovered which could affect the content, and all legal disclaimers that apply to the journal pertain.

1 **Influence of bromine and iodine chemistry on annual, seasonal, diurnal, and background**
2 **ozone: CMAQ simulations over the Northern Hemisphere**

3
4
5
6 Golam Sarwar¹, Brett Gantt², Kristen Foley¹, Kathleen Fahey¹, Tanya L. Spero¹, Daiwen Kang¹,
7 Rohit Mathur¹, Hosein Foroutan³, Jia Xing⁴, Tomás Sherwen^{5,6}, Alfonso Saiz-Lopez⁷
8
9
10

11
12 ¹National Exposure Research Laboratory, US Environmental Protection Agency, RTP, North Carolina 27711, USA
13

14 ²Office of Air Quality Planning and Standards, US Environmental Protection Agency, RTP, NC 27711, USA
15

16 ³The Charles E. Via, Jr. Department of Civil & Environmental Engineering, Virginia Tech, Blacksburg 24061, USA
17

18 ⁴State Key Joint Laboratory of Environmental Simulation and Pollution Control, School of Environment, Tsinghua
19 University, Beijing 100084, China
20

21 ⁵Wolfson Atmospheric Chemistry Laboratories, Department of Chemistry, University of York, UK
22

23 ⁶National Centre for Atmospheric Science, Department of Chemistry, University of York, UK
24

25 ⁷Department of Atmospheric Chemistry and Climate, Institute of Physical Chemistry Rocasolano, CSIC, Madrid
26 28006, Spain
27
28
29
30
31
32
33
34
35
36
37
38
39
40
41
42
43
44
45
46
47

48 **Corresponding author:* Golam Sarwar, US EPA, 109 T.W. Alexander Drive, Research Triangle Park, NC 27711, USA;
49 Tel.: 919-541-2669; fax: 919-541-1379; e-mail: sarwar.golam@epa.gov

50 **ABSTRACT**

51 Bromine and iodine chemistry has been updated in the Community Multiscale Air Quality
52 (CMAQ) model to better capture the influence of natural emissions from the oceans on ozone
53 concentrations. Annual simulations were performed using the hemispheric CMAQ model
54 without and with bromine and iodine chemistry. Model results over the Northern Hemisphere
55 show that including bromine and iodine chemistry in CMAQ not only reduces ozone
56 concentrations within the marine boundary layer but also aloft and inland. Bromine and iodine
57 chemistry reduces annual mean surface ozone over seawater by 25%, with lesser ozone
58 reductions over land. The bromine and iodine chemistry decreases ozone concentration without
59 changing the diurnal profile and is active throughout the year. However, it does not have a strong
60 seasonal influence on ozone over the Northern Hemisphere. Model performance of CMAQ is
61 improved by the bromine and iodine chemistry when compared to observations, especially at
62 coastal sites and over seawater. Relative to bromine, iodine chemistry is approximately four
63 times more effective in reducing ozone over seawater over the Northern Hemisphere (on an
64 annual basis). Model results suggest that the chemistry modulates intercontinental transport and
65 lowers the background ozone imported to the United States.

66

67

68 **Keywords:** bromine, iodine, ozone, background ozone, CMAQ

69

70 1.0 INTRODUCTION

71 Although anthropogenic emissions of nitrogen oxides (NO_x) and volatile organic compounds
72 (VOC) within the United States (U.S.) have a large influence on ambient surface ozone (O_3)
73 concentrations, other processes such as natural emissions, stratospheric intrusions, and long-
74 range transport can affect surface O_3 concentrations at some locations within the U.S. Among
75 these natural emissions are chemical compounds from the ocean surface that can reduce
76 atmospheric O_3 concentrations through catalytic reactions. Bromine reactions deplete O_3 in the
77 tropical marine boundary layer (Dickerson et al., 1999) and when combined with iodine
78 reactions, they can deplete O_3 much faster than would have been expected if they acted
79 individually (Saiz-Lopez et al., 2007; Mahajan et al., 2010). Bromine and iodine are produced in
80 the ocean through both biotic and abiotic pathways resulting in measurable concentrations of
81 both organic and inorganic species within the marine boundary layer. Several modeling studies
82 have implemented marine bromine and iodine emission sources and chemistry with increasing
83 levels of scope, ranging from one-dimensional models (e.g. von Glasow, et al., 2002a; von
84 Glasow, et al., 2002b) to global chemical transport models (e.g. Ordóñez, et al., 2012; Saiz-
85 Lopez et al., 2012; Saiz-Lopez et al., 2014; Fernandez et al., 2014; Sherwen et al., 2016a;
86 Sherwen et al., 2016b).

87
88 A disconnect between anthropogenic precursor emissions and surface O_3 concentrations at some
89 U.S. sites has led to an increased focus on background O_3 (Fiore et al., 2002; Fiore et al., 2003;
90 Fiore et al., 2014). The U.S. Environmental Protection Agency (EPA) considers background O_3
91 to be any O_3 formed from sources or processes other than U.S. manmade emissions of NO_x ,
92 VOC, methane, and carbon monoxide (EPA, 2016). Previous photochemical modeling studies

93 (Parrish et al., 2009; Cooper et al., 2010; Zhang et al., 2011; McDonald-Buller et al., 2011)
94 which estimated the contribution of background sources on U.S. O₃ concentrations have found
95 that (1) seasonal mean background concentrations are highest in the Intermountain West, (2)
96 seasonal mean background concentrations are generally highest in the Spring and early Summer,
97 (3) background impacts can occur on episodic and non-episodic scales, and (4) air quality
98 models are not capable of estimating background values accurately on a daily basis.

99
100 Background O₃ levels in coastal areas are affected by marine boundary layer chemistry, which is
101 influenced by atmosphere-ocean interactions. Several previous studies examined the impacts on
102 O₃ by bromine (e.g. Ordóñez, et al., 2012; Fernandez et al., 2014; Yang et al., 2005; Parrella et
103 al., 2012; Schmidt et al., 2016; Breton et al. 2017) and iodine chemistry (e.g. Saiz-Lopez et al.,
104 2014; Sherwen et al., 2016a; Sherwen et al., 2016b; McFiggans et al., 2000; Long et al., 2014;
105 Badia et al., 2017) using air quality models. Sarwar et al. (2015), Gantt et al. (2017), and Muñiz-
106 Unamunzaga et al. (2018) showed that including marine bromine and iodine chemistry in the
107 Community Multiscale Air Quality (CMAQ) model not only reduces summertime marine
108 boundary layer O₃ concentrations by more than 5 ppbv, but also reduces O₃ in the free
109 troposphere and inland areas far from the coast. In this study, we refine the marine bromine and
110 iodine chemistry in the CMAQ model and extend the simulations to examine its influence on
111 annual, seasonal, diurnal, and background O₃.

112

113 **2.0 METHODOLOGY**

114 CMAQ is a 3-D chemical transport model containing comprehensive treatments of many
115 important atmospheric processes and is widely used for both regulatory and research purposes

116 (e.g. Appel et al., 2013; Appel et al., 2017; Ring et al., 2018; Qiao et al., 2018). We use the
117 hemispheric version (Mathur et al., 2017) of CMAQ version 5.2 (www.epa.gov/cmaq) to
118 simulate the year 2006 with meteorological fields generated from the Weather Research and
119 Forecasting (WRFv3.8.1) model employing the Thompson microphysics option (Skamarock et
120 al., 2008). WRF results were further processed using the Meteorology Chemistry Interface
121 Processor (Otte and Pleim, 2010) (MCIPv4.3) to prepare CMAQ-ready meteorological files. The
122 model vertical extent reaches to 50 hPa containing 44 layers of varying thickness and uses 108-
123 km horizontal grid spacings. The surface layer has a thickness of 20 meters.

124
125 The 2005 Carbon Bond chemical mechanism (CB05e51) containing updated toluene, oxidized
126 nitrogen, and isoprene reactions (Appel et al., 2017) is combined with the chlorine (Sarwar et al.,
127 2012), bromine, and iodine chemistry for this study. Sarwar et al. (2015) incorporated an initial
128 version of bromine and iodine chemistry into CMAQ and examined its lower and upper limits of
129 the impacts on O₃. The upper limit included photolysis of higher iodine oxides while the lower
130 limit did not. The model without the photolysis of iodine oxides yielded lesser reduction of O₃
131 over seawater (15%) compared to the model with the photolysis of iodine oxides which reduced
132 O₃ by 48%. Since this 48% reduction resulted in unrealistically low O₃ concentrations in Sarwar
133 et al. (2015), photolysis rates of higher iodine oxides have not been included in any publicly
134 available version of the CMAQ model. Sarwar et al. (2015) also included one heterogeneous
135 reaction of bromine nitrate.

136
137 In this study, the CMAQ bromine and iodine chemistry described in Sarwar et al. (2015) is
138 further improved to include photolysis of higher iodine oxides (Table S1-S2), several

139 heterogeneous reactions of bromine and iodine species (Table S3) with aerosol chloride (Cl^-) and
140 bromide (Br^-), and refined bromine and halocarbon emissions. In the previous CMAQ model,
141 photolysis rates of higher iodine oxides were calculated using absorption cross-section and
142 quantum yield from Saiz-Lopez et al. (2014). Sherwen et al. (2016a) used absorption cross-
143 section and quantum yield of iodine nitrate for calculating photolysis rates of higher iodine
144 oxides which is now used in the CMAQ model.

145
146 We also incorporate several aqueous-phase reactions of bromine species following Long et al.
147 (2013) (Table S4). Cloud chemistry of bromine species was added to the CMAQ cloud module
148 “AQCHEM-KMT” (Fahey et al. 2017) using the Kinetic PreProcessor (KPP) v.2.2.3 (Damian et
149 al. 2002). AQCHEM-KMT simulates the evolution of species in and around cloud water by
150 calculating kinetic mass transfer between gas and aqueous phases, interstitial aerosol scavenging,
151 dissociation of ionic species, aqueous phase chemical reactions, and wet deposition.

152
153 Sarwar et al. (2015) used halocarbon, inorganic bromine, and inorganic iodine emissions in the
154 CMAQ model, the rates of which are refined in this study. For halocarbon species, the emission
155 rates are calculated following the procedures of Ordóñez et al. (2012) and Yarwood et al. (2012):

$$156 \quad E_{\text{HC}} = E_{\text{base}} \times (O_{\text{F}} + S_{\text{F}}) \times A_{\text{GC}} \times f_{\text{HC}} \times f_{\text{DP}} \times \text{chl-}a \quad (1)$$

157
158
159 where, E_{HC} is the halocarbon emission rates (moles s^{-1}), E_{base} represents the halocarbon base
160 emission rate (moles s^{-1}), O_{F} is the open ocean fraction of a grid cell, S_{F} is the surf zone fraction
161 of a grid cell, A_{GC} is the grid cell area (m^2), f_{HC} is a species-dependent emission factor, f_{DP} is a

162 diurnal profile factor, and chl-*a* is the monthly climatological chlorophyll value (mg m^{-3}) from
163 the Moderate Resolution Imaging Spectroradiometer (MODIS).

164
165 In Sarwar et al. (2015), chl-*a* values were capped at 1.0 following Yarwood et al. (2012); in this
166 study, we used the actual chl-*a* values from MODIS which can be greater than 1.0 in coastal
167 areas. This change in chl-*a* values necessitated a revision in the base emission rate from 1.2×10^{-11}
168 in Sarwar et al. (2015) to 6.9×10^{-12} to replicate the global estimates of halocarbon emissions
169 reported by Ordóñez et al. (2012). This revision was done outside the CMAQ framework by
170 using the native MODIS derived global land/ocean grid areas and chl-*a* values. We iterated the
171 base emission rate until suitable agreement with the Ordóñez et al. (2012) estimates was reached.

172 The use of the revised base emission rate and the actual chl-*a* values reduces the total
173 hemispheric halocarbon emissions estimates by ~20% compared to the estimates of Sarwar et al.
174 (2015). It also changes the allocation of halocarbon emissions to different grid-cells. More
175 halocarbon emissions are now allocated to coastal areas and less are allocated to open oceans
176 compared to the estimates of Sarwar et al. (2015).

177
178 Refinement of the inorganic emissions included the replacement of the simplified treatment of
179 directly emitting inorganic bromine emissions (Yang et al., 2005 and Sarwar et al., 2015) with
180 the physically-based heterogeneous chemistry of bromine and iodine species (Table S3)
181 following Fernandez et al. (2014) and Sherwen et al. (2016b). This required a revision to the sea
182 spray emissions in CMAQ (Gantt et al., 2015) to include Br^- in the chemical speciation.

183 Specifically, the sea spray emissions are speciated by mass (gm/gm) following Millero (1996):
184 $\text{Cl}^- = 0.5528$, $\text{Na}^+ = 0.3080$, $\text{SO}_4^{2-} = 0.0775$, $\text{Ca}^{2+} = 0.0118$, $\text{Mg}^{2+} = 0.0367$, $\text{K}^+ = 0.0113$, and Br^-
185 $= 0.0019$. We also updated the minimum wind speed in the inorganic iodine emissions

186 parameterization (McDonald et al., 2014) from 3 m s^{-1} in Sarwar et al. (2015) to 5 m s^{-1}
 187 following the value used for the GEOS-Chem model (Sherwen et al., 2016a) which reduces the
 188 emissions estimates by ~15%. Hemispheric halocarbon and inorganic iodine emission rates,
 189 along with global estimates reported in previous studies, are shown in Table 1. Generally, our
 190 halocarbon emissions estimates for the Northern Hemisphere are lower than the reported global
 191 estimates while inorganic iodine emissions estimates fall between the reported ranges of global
 192 estimates.

193

194 Table 1: Halocarbon and inorganic iodine emissions estimates

Species	Hemispheric annual estimates in this study (Gg)	Global annual estimates from published studies (Gg)
CHBr_3	301	533
CH_2Br_2	51.5	67.3
CH_2BrCl	6.1	10.0
CHBr_2Cl	14.8	19.7
CHBrCl_2	14.5	22.6
CH_3I	135	303
CH_2ICl	148	234
CH_2IBr	54.4	87.3
CH_2I_2	73	116
$\text{HOI} + 2\text{xI}_2$	2052	1,900 – 3,230

195 Note: Global annual estimates of halocarbon emissions are taken from Ordóñez et al. (2012), global annual
 196 estimates of $\text{HOI} + 2\text{xI}_2$ are taken from Saiz-Lopez et al. (2014) and Sherwen et al. (2016a)

197

198

199 We performed six annual simulations for this study that can be grouped in three pairs. In the first

200 pair, one simulation used CB05e51 along with the chlorine chemistry (hereto referred as

201 “No_Br/I”), while the other added bromine and iodine chemistry (“Added_Br/I”). A second set

202 of simulations was completed to investigate the influence of the bromine and iodine chemistry

203 independently. In this second pair, one simulation added only bromine chemistry updates

204 (“Added_Br”) while the other added only iodine chemistry updates (“Added_I”). The final set of

205 simulations was completed to investigate the impact of bromine and iodine chemistry on

206 background O_3 over the U.S. For the third pair, the model chemistry was identical to the first pair

207 but with anthropogenic emission sources over North America were zeroed out
208 (“No_Br/I_NoAnth” and “Added_Br/I_NoAnth”, respectively). All the annual simulations were
209 completed with a three-month spin-up period (October – December of 2005) and initialized from
210 previous model results (Xing et al., 2016).

211

212 **3.0 RESULTS AND DISCUSSION**

213

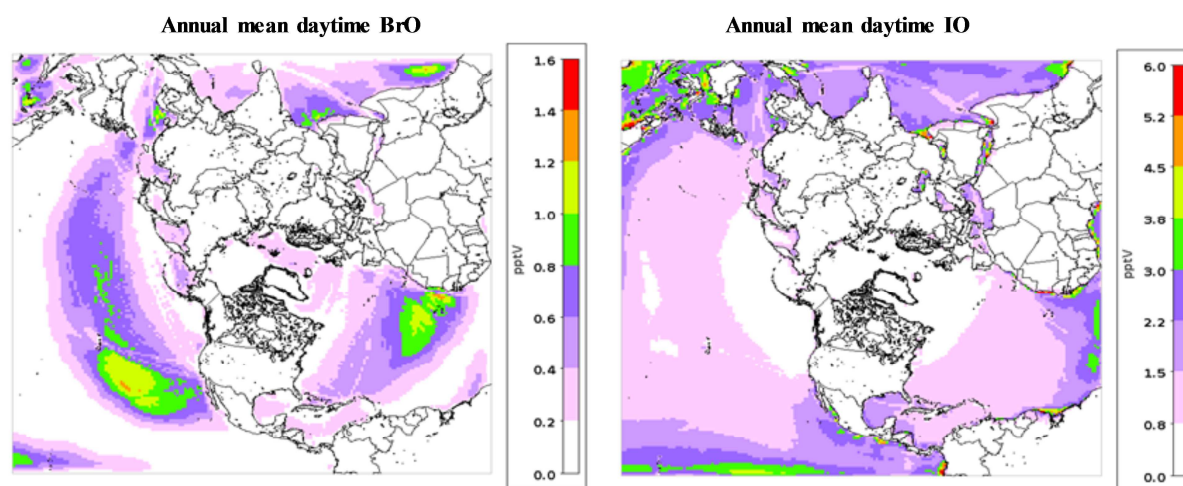
214 **3.1 Predicted BrO (bromine monoxide) and IO (iodine monoxide)**

215 BrO and IO are reaction products of the bromine and iodine chemistry. Annual mean daytime
216 BrO and IO concentrations are shown in Figure 1. BrO concentrations of 0-0.8 pptv are predicted
217 over large oceanic areas. However, higher values (>0.8 pptv) are also predicted over limited
218 areas of mid-latitude oceans. In contrast, IO concentrations of 0-3.0 pptv are predicted over large
219 oceanic areas and higher values (>3.0 pptv) are predicted only over limited oceanic areas.

220 The current bromine/iodine chemistry enhances BrO and IO levels compared to the previous
221 version of the chemistry without the photolysis of higher iodine oxides in CMAQ (Sarwar et al.,
222 2015). For example, predicted summertime BrO levels with the previous version rarely exceed
223 0.5 pptv over the mid-latitude oceanic areas. In contrast, predicted BrO levels with the current
224 version exceed 1.0 pptv over large portions of the mid-latitude oceanic areas. Overall, the current
225 chemistry increases surface BrO levels by a factor of ~2.0 averaged over the entire seawater.

226 Predicted summertime IO levels over most areas of seawater range from 0.5-1.5 pptv and 0.5-3.0
227 pptv for the previous and current versions of the chemistry, respectively. Overall, the current
228 chemistry increases surface IO levels by a factor of ~1.5 averaged over the entire seawater. The
229 BrO enhancement occurs primarily due to the inclusion of aqueous-phase and heterogeneous

230 reactions while the IO enhancement occurs due to the inclusion of photolysis of higher iodine
 231 oxides and the heterogeneous reactions.



232
 233 Figure 1. Simulated annual mean daytime surface BrO and IO concentrations with the bromine and iodine chemistry
 234 (Added_Br/I). Annual mean concentrations were multiplied by 2.0 to estimate approximate annual mean daytime
 235 BrO and IO concentrations.

236
 237 We compare model predictions with published values from different years for an approximate
 238 evaluation of the bromine and iodine chemistry in CMAQ. Predicted BrO levels are lower than
 239 observed values at all locations (Table 2). CMAQ predicted values are also lower than ground-
 240 based daytime BrO measurements of <0.5-2.0 pptv and ship-based daytime BrO measurements
 241 of <~3.0-3.6 pptv (Saiz-Lopez et al., 2012). Thus, CMAQ generally under-predicts BrO levels.
 242 In contrast, CMAQ predicted values are similar to observed IO levels at Cape Verde Islands;
 243 Tenrife, Spain; Dagebüll, Germany but are lower than observed values at Brittany, France and
 244 Mace Head, Ireland (Table 2). Dix et al. (2013) measured IO concentrations over the Pacific
 245 Ocean in January of 2010 and reported an average value of 0.5 pptv inside the marine boundary
 246 layer. CMAQ predicted surface layer values range from 0.4 to 1.0 pptv over the region. Saiz-
 247 Lopez et al. (2012) reported that ground-based daytime IO measurements range from <0.2 to 2.4

248 pptv while ship-based daytime IO measurements range ~3.5 pptv. CMAQ predicted IO levels are
 249 similar to these reported observed values. Thus, CMAQ generally captures observed IO values.

250

251 Table 2: A comparison of observed daytime BrO and IO concentrations with CMAQ predictions

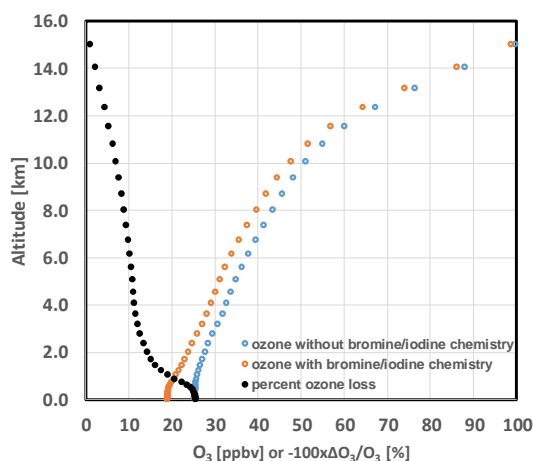
Location	Species	Observed value (pptv)	Predicted value (pptv)
Cape Verde Islands ^a	BrO	2.8	0.7
Dagebüll, Germany ^b	BrO	0.4	0.1
Brittany, France ^b	BrO	1.5	0.03
Mace Head, Ireland ^c	BrO	2.3	0.05
Cape Verde Islands ^a	IO	1.5	1.2
Dagebüll, Germany ^b	IO	0.7	0.8
Brittany, France ^b	IO	1.5	0.2
Mace Head, Ireland ^d	IO	1.2	0.14
Tenrife, Spain ^d	IO	1.2	1.1

252 Note: a - Mahajan et al., 2010; b - Peters et al., 2005; c - Saiz-Lopez et al., 2006; d - Allan et al., 2000. Cape Verde values represent daytime
 253 average of long-term measurements; CMAQ predicted annual daytime mean values are compared. Values at other locations represent daytime
 254 average over campaign; CMAQ predicted monthly daytime mean values are compared. Peters et al. (2005) reported average values for the entire
 255 campaign which we multiplied by 2.0 to estimate daytime average values.

256

257 3.2 Influence on annual mean O₃

258 Annual mean surface O₃ concentration over seawater without bromine and iodine chemistry is
 259 ~25 ppbv and increases with altitude (Figure 2). Consistent with the results of Sherwen et al.,
 260 (2016b), the bromine and iodine chemistry reduces mean surface O₃ over seawater by 25% and
 261 reduces O₃ throughout the lower troposphere. Such reduction occurs due primarily to the
 262 reactions of O₃ with bromine and iodine radicals generated from photolysis and reactions of
 263 halocarbons and inorganic bromine and iodine species with hydroxyl radical. The influence of
 264 bromine and iodine chemistry on O₃ decreases with altitude and is negligible at ~15 km. Saiz-
 265 Lopez et al. (2014) and Sarwar et al. (2015) reported lower and upper limits (17-27% and 15-
 266 48%) of the impacts on O₃; and the O₃ changes reported in this study fall within their published
 267 ranges.

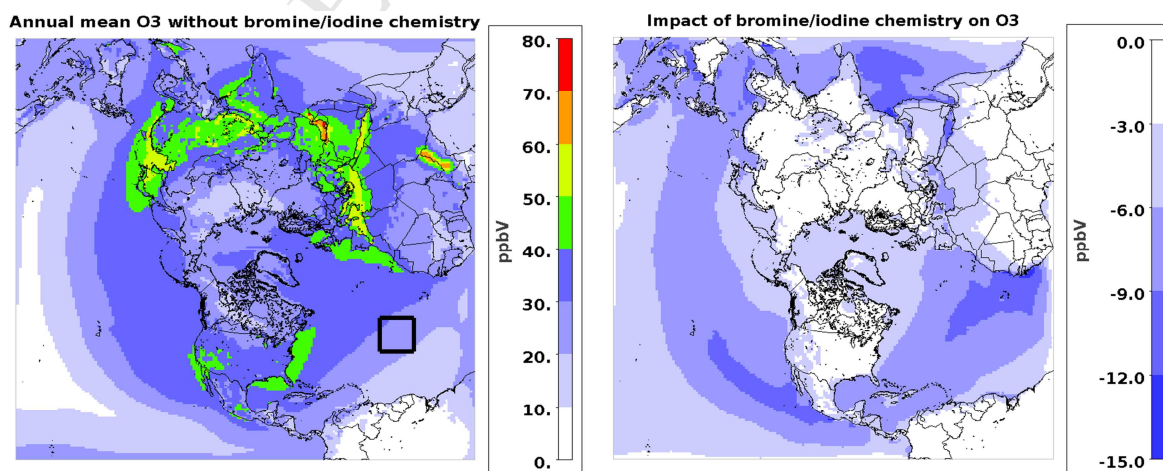


268

269 Figure 2. Simulated annual mean O_3 over seawater in the Northern Hemisphere without (No_Br/I) and with the
 270 bromine and iodine chemistry (Added_Br/I) and annual mean percent reduction of O_3 by the bromine and iodine
 271 chemistry [$100 \times (\text{Added_Br/I} - \text{No_Br/I}) / \text{No_Br/I}$]
 272

273 The spatial distribution of the annual mean O_3 without bromine and iodine chemistry is shown in
 274 Figure 3a with the highest values over portions of Asia, Africa, and the western U.S. and lower
 275 values predicted over seawater (especially over remote oceanic areas). The inclusion of bromine
 276 and iodine chemistry reduces surface O_3 by 3-12 ppbv over large areas of seawater (Figure 3b)
 277 and by 3-6 ppbv in many coastal areas including the Pacific, Gulf of Mexico, and Atlantic coasts.
 278 Its impact on O_3 over land is smaller than that over seawater, although all areas of the U.S. have
 279 a predicted ~ 2 ppbv or greater reduction in O_3 from the bromine and iodine chemistry.

280



281

282 Figure 3. (a) Annual mean surface O₃ without the bromine and iodine chemistry (No_Br/I) (b) influence of the
283 bromine and iodine chemistry on annual mean O₃ (Added_Br/I - No_Br/I). Black square box is the area over which
284 diurnal, day-to-day, and monthly variations are calculated as shown in Figure 4 and 5.

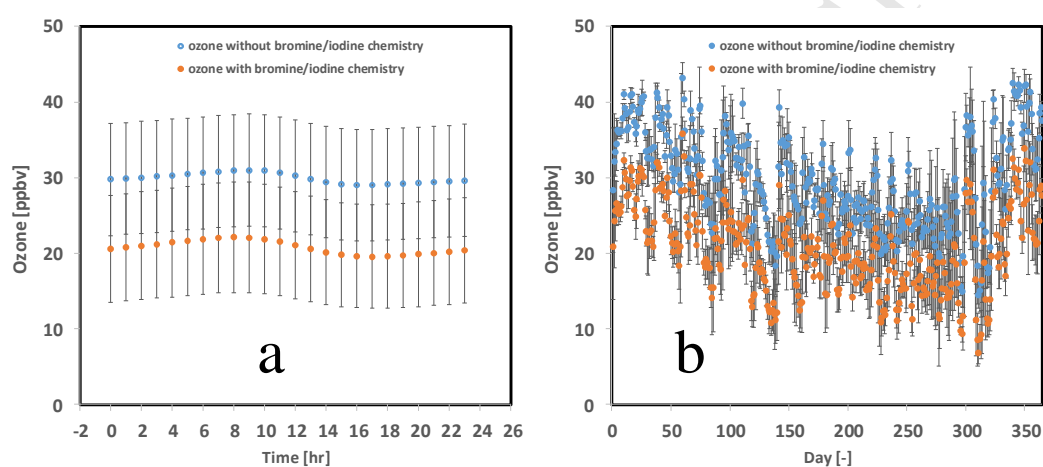
285
286 The bromine and iodine chemistry in this study is more efficient in reducing O₃ over seawater
287 compared to the previous version of the chemistry without the photolysis of higher iodine oxides
288 in CMAQ (Sarwar et al., 2015). For example, the previous chemistry reduces summer-time O₃
289 over seawater generally by 2-8 ppbv while the current chemistry reduces O₃ over seawater by 3-
290 12 ppbv. Both versions of the bromine and iodine chemistry have similar impacts over land
291 areas.

293 3.3 Influence on diurnal variation of O₃

294 To examine the influence of the bromine and iodine chemistry on the diurnal variation of O₃, we
295 calculated a mean diurnal profile for an area over the Atlantic Ocean (see Figure 3a) by
296 averaging across all days in the annual simulation for each hour of the day, as shown in Figure
297 4a. The area is selected to minimize the influence of anthropogenic emissions on O₃. Predicted
298 O₃ levels with the bromine and iodine chemistry are lower (by 7-8 ppbv) than those in
299 simulations without the bromine and iodine chemistry. There is a pronounced diurnal cycle in
300 both simulations, as O₃ concentrations increase from midnight and peak in the morning, then
301 decrease to a minimum value in the afternoon before increasing again. This diurnal variation
302 results from low concentrations of O₃ precursors over remote areas of seawater that limit O₃
303 production as has been previously reported by Read et al. (2008). In contrast, the O₃ levels over
304 land typically peak in the afternoon due to the higher concentrations of O₃ precursors (David and
305 Nair, 2011). When bromine and iodine chemistry are excluded, O₃ is reduced primarily by the
306 photolysis of O₃ and its reaction with hydroperoxy radical (HO₂). Adding bromine and iodine

307 chemistry creates more pathways to O_3 reduction. Thus, the bromine and iodine chemistry
 308 reduces O_3 ; however, it does not alter the diurnal profile of O_3 . While the diurnal cycle of O_3
 309 without the bromine and iodine chemistry varies slightly with locations due to precursors,
 310 meteorology and other factors, the bromine and iodine chemistry does not alter the diurnal cycle
 311 at any location but rather simply reduces O_3 concentrations.

312



313

314 Figure 4. (a) Influence of the bromine and iodine chemistry on diurnal variation of surface O_3 (b) influence of the
 315 bromine and iodine chemistry on the day-to-day variation of surface O_3 . Blue circle – No_Br/I and red circle –
 316 Added_Br/I.

317

318 3.4 Influence on the day-to-day variation of O_3

319 To examine the day-to-day variation of the bromine and iodine chemistry impacts on O_3 , we first
 320 calculated daily-mean O_3 values for each grid cell over seawater. We then calculated a mean
 321 daily value from the same area over the Atlantic Ocean (see Figure 3a). Bromine and iodine
 322 chemistry reduces O_3 on each day of the year (Figure 4b), but the magnitude of the reduction
 323 varies from day to day. Such variation depends on multiple factors including existing
 324 atmospheric O_3 levels and wind speed. The O_3 levels can influence the daily variation in two
 325 ways: 1) higher O_3 concentrations increase inorganic iodine emissions which react with and

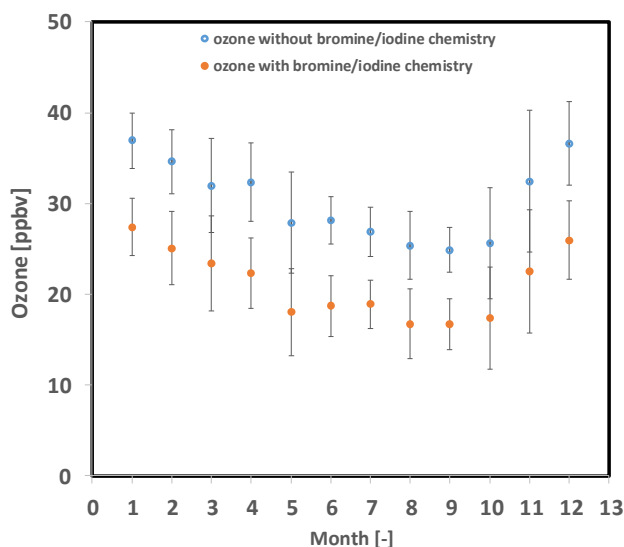
326 reduce O₃ and 2) higher O₃ increases the reaction rates with bromine and iodine which reduces
327 O₃. Wind speed can influence the daily variation in two ways: 1) lower wind speed enhances
328 inorganic iodine emissions (McDonald et al., 2014) which further reduce O₃ and 2) lower wind
329 speed increases available reaction time between O₃ and bromine/iodine species which can also
330 reduce additional O₃. Bromine and iodine chemistry most efficiently reduces O₃ at low wind
331 speeds and high existing O₃ concentrations.

332

333 **3.5 Seasonal variation of the influence on O₃**

334 To examine the seasonal variation of the bromine and iodine chemistry impacts on O₃, we first
335 calculated monthly mean O₃ from daily-mean values for each grid cell over seawater. We then
336 calculated a mean value from the same area over the Atlantic Ocean (see Figure 3a). Mean O₃
337 levels are highest in cooler months and lowest in warmer months (Figure 5) due to the low O₃
338 precursor levels over seawater that limit O₃ production and cause loss processes to control O₃
339 concentrations. Photolysis of O₃ and its reaction with HO₂ are two dominant loss processes over
340 seawater (Breton et al., 2017). The loss via photolysis is highest in warmer months due to high
341 actinic flux. Atmospheric HO₂ levels are high in warmer months due to higher photochemical
342 activity; thus, the loss of O₃ via its reaction with HO₂ is also high in warmer months. Bromine
343 and iodine chemistry reduces monthly mean O₃ by ~8-10 ppbv. The reduction of O₃ from
344 bromine and iodine chemistry is largest in December and lowest in July. Bromine and iodine
345 chemistry reduces seasonal mean surface O₃ in Winter (December-February) by 9.9 ppbv, Spring
346 (March-May) by 9.5 ppbv, Summer (June-August) by 8.7 ppbv, and Fall (September-November)
347 by 8.8 ppbv. If the entire seawater is considered, bromine and iodine chemistry reduces mean
348 surface O₃ over seawater by 6.9 ppbv, 6.8 ppbv, 5.9 ppbv, and 6.2 ppbv in Winter, Spring,
349 Summer, and Fall, respectively. Slightly greater O₃ losses occur in the Winter and Spring seasons

350 due primarily to the bromine chemistry and the fact that lower temperatures in cooler months
 351 promote efficient partitioning of hydrobromic acid into Br^- which enhances heterogeneous
 352 production of ozone-reacting bromine species.
 353



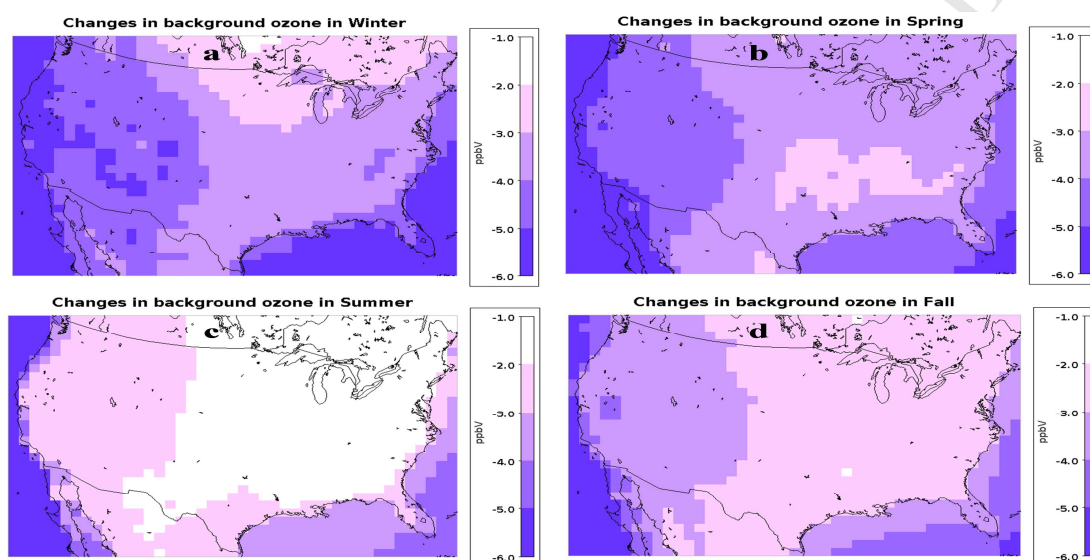
354
 355 Figure 5. Influence of the bromine and iodine chemistry on month-to-month variation of surface O_3 . Error bars are
 356 represented with two standard deviation. Blue circle – No_Br/I and orange circle – Added_Br/I
 357
 358

359 3.6 Influence on background O_3

360 By comparing the pair of simulations with anthropogenic emission sources over North America
 361 zeroed out, we are able estimate the impact of iodine and bromine chemistry on background O_3
 362 over North America. The bromine and iodine chemistry reduces seasonal mean background O_3
 363 over the U.S. in all seasons (Figure 6) with the greatest reduction occurring in the Winter and
 364 Spring (2-6 ppbv) followed by the Fall (2-4 ppbv) and Summer (1-3 ppbv). For all seasons,
 365 bromine and iodine chemistry reduces more O_3 over the western U.S. and coastal areas than over
 366 other inland areas, which is consistent with the results shown in Figure 3b. The springtime
 367 reductions in the western U.S. are in areas that have some of the highest background O_3

368 concentrations in the U.S. (Dolwick, et al., 2016). These substantial reductions in background O_3
 369 from the bromine and iodine chemistry suggest that atmospheric models without this chemistry
 370 potentially overpredict background O_3 . Our results corroborate the findings of Wang et al. (2015)
 371 who reported that halogen chemistry affects the intercontinental transport of O_3 .

372



373

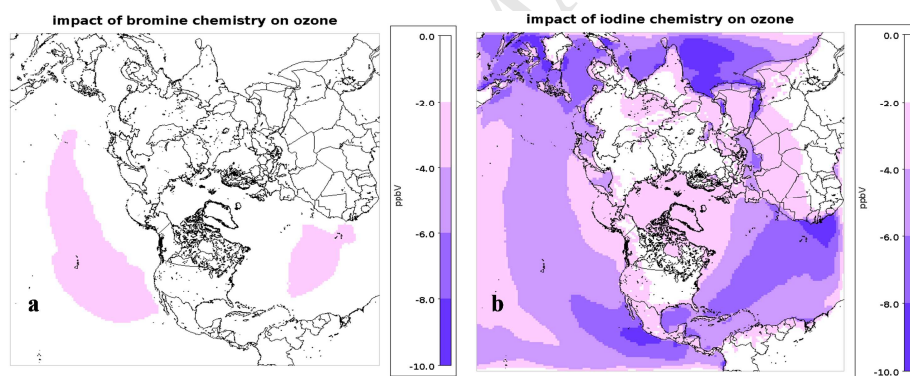
374 Figure 6. Influence of the bromine and iodine chemistry (Added_Br/I_NoAnth – No_Br/I_NoAnth) on seasonal
 375 mean background O_3 over the U.S. (a) Winter (b) Spring (c) Summer (d) Fall. Winter: December- February;
 376 March-May; Summer: June-August; Fall: September-November.
 377

378 3.7 Isolating the impacts of bromine and iodine chemistry on O_3

379 Figure 7 shows that bromine and iodine chemistry have different impacts on O_3 concentrations;
 380 bromine chemistry reduces annual mean surface O_3 over limited areas of seawater by 2-4 ppbv
 381 (Figure 7a) while the iodine chemistry reduces O_3 by 2-10 ppbv over most oceanic areas (Figure
 382 7b). Iodine chemistry affects model prediction over the entire U.S. and reduces annual mean O_3
 383 by 1-2 ppbv over the eastern U.S., 2-3 ppbv over the western U.S., and 3-4 ppbv over some
 384 coastal areas. In contrast, bromine chemistry reduces annual mean O_3 by <1 ppbv over U.S. On
 385 average, bromine chemistry reduces annual mean O_3 over seawater by 1.2 ppbv while iodine

386 chemistry reduces O_3 by 5.2 ppbv. Iodine chemistry is more efficient in reducing O_3 than the
 387 bromine chemistry due to several factors. The rate constant for the $I + O_3$ reaction is ~10%
 388 greater than that of the $Br + O_3$ reaction (Ordóñez, et al., 2012). Iodine recycles at a faster rate
 389 than bromine due to higher photolysis rates of I_2/HOI compared to $Br_2/HOBr$ as well as the
 390 presence of higher iodine oxides in the model. Additionally, the inorganic iodine emissions rates
 391 are a function of dissolved O_3 and iodide present in seawater (Carpenter et al., 2013) and are
 392 higher when atmospheric O_3 concentrations are higher. Such factors in iodine chemistry reduce
 393 O_3 over seawater more efficiently than that of bromine chemistry. Lower O_3 concentrations over
 394 the marine environment due to iodine chemistry are transported inland resulting in lower O_3 over
 395 land.

396



397

398 Figure 7. Changes in annual mean surface O_3 with (a) bromine chemistry (Added_Br – No_Br/I) and (b) iodine
 399 chemistry (Added_I – No_Br/I)

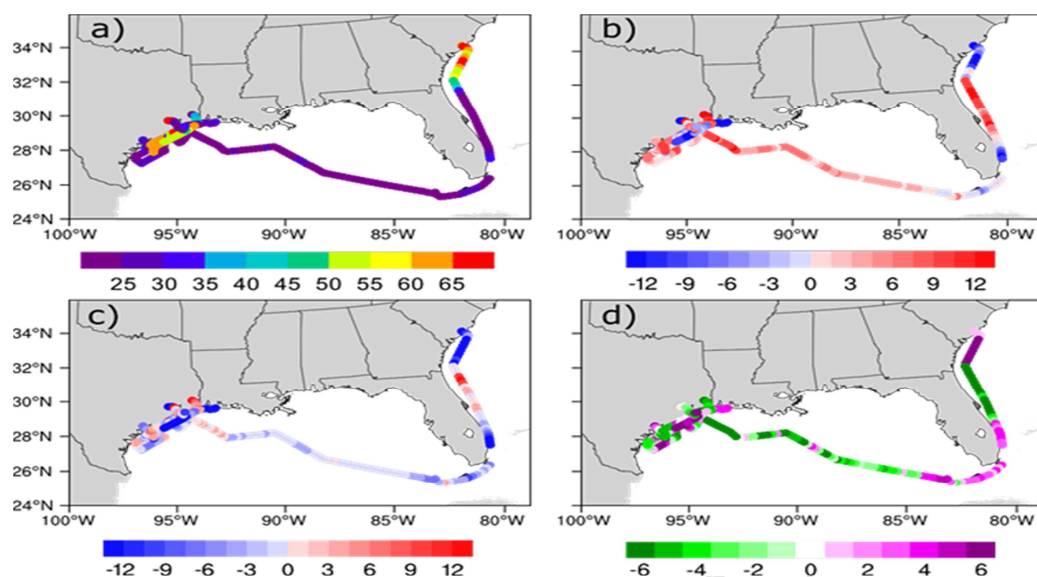
400

401 3.8 Influence of iodine and bromine chemistry on O_3 model performance

402 In addition to the direct comparison between model simulations, we have also evaluated the
 403 simulations without and with bromine and iodine chemistry against both ship-based and land-
 404 based O_3 observations. The ship-based surface measurements used for this evaluation are over
 405 the Gulf of Mexico from the 2006 Texas Air Quality Study (Parrish et al., 2009b) (TexAQS).

406 Observed O₃ concentrations during the August 2006 period of the TexAQS campaign are
407 generally less than 30 ppbv, though higher values were measured over some coastal waters off
408 Texas, South Carolina and Georgia (Figure 8a). Model mean bias values (Figure 8b-c) show that
409 neither model simulation captures the high observed values near some coastal waters which
410 results in a negative bias. The model without the bromine and iodine chemistry, however, has a
411 positive bias (median bias +4.7 ppbv) over most areas in the remote ocean while the model with
412 the bromine and iodine chemistry typically has a slight negative bias (median bias -1.0 ppbv,
413 95% of the observations have a bias within ± 30 ppbv) for these areas. We also compared the
414 performance of the simulations without and with bromine and iodine chemistry by calculating
415 the difference in the absolute mean bias between the two simulations. In this calculation, positive
416 values mean that the simulation with bromine and iodine chemistry has a higher absolute bias
417 (further from observations) while negative values indicate that it has a lower absolute bias (closer
418 to observations). The difference in absolute mean bias shown in Figure 8d reveals that the
419 inclusion of bromine and iodine chemistry generally reduces the bias by 2-6 ppbv over the ocean
420 without much degradation in other regions.

421



422

423 Figure 8. (a) Observed surface O_3 concentrations from R/V Ronald H. Brown during August 2006 of the TexAQS
 424 campaign (Parrish et al., 2009b) (b) model mean bias for the model without any bromine and iodine chemistry
 425 (No_Br/I – Observations) (c) model mean bias for the model with the bromine and iodine chemistry (Added_Br/I –
 426 Observations), and (d) differences in the model absolute mean bias between simulations without and with bromine
 427 and iodine chemistry ($|Added_Br/I - Observations| - |No_Br/I - Observations|$). The green colors in (d) represent
 428 locations where the simulation with the bromine and iodine chemistry had a lower model bias (improved prediction),
 429 and purple colors represent locations where the simulation with the bromine and iodine chemistry had a higher
 430 model bias (worse prediction). All units are in ppbv.

431
432
433

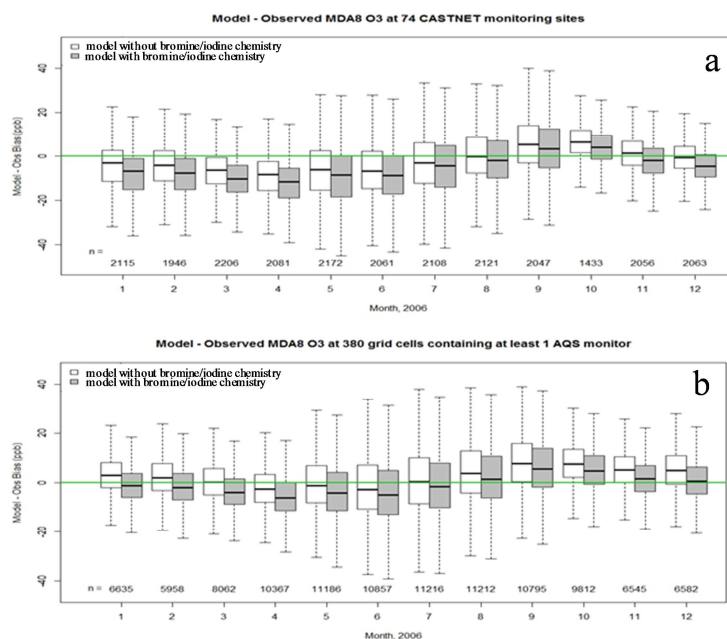
434 The simulations without and with bromine and iodine chemistry were also evaluated against
 435 observations in the U.S. from the Clean Air Status and Trends Network (CASTNET) and the
 436 USEPA's Air Quality System (AQS). CASTNET and AQS include sites at mainly remote and
 437 mainly urban locations, respectively. Monthly mean bias for the simulation without the bromine
 438 and iodine chemistry varies (-8 to +4 ppbv for CASTNET sites and -3 to +7 ppbv for AQS sites),
 439 with negative biases (underprediction) for several months (January - August and December at
 440 CASTNET sites and April – June for AQS sites) and positive biases (overprediction) for other
 441 months (Figure 9). The inclusion of bromine and iodine chemistry generally improves O_3
 442 predictions in the Fall at both the CASTNET and AQS sites and deteriorates the model
 443 predictions in the Spring. In the Winter and Summer, the simulation with bromine and iodine

444 chemistry generally has degraded predictions at the CASTNET sites and improved predictions at
445 the AQS sites.

446

447 When only the coastal sites are considered, the monthly mean biases for the simulation without
448 bromine and iodine chemistry are positive for January – February and July - December at
449 CASTNET sites (Figure 10a) and for all months at AQS sites (Figure 10b). Differences between
450 the simulations without and with bromine and iodine chemistry are more noticeable for the
451 coastal sites, with a larger number of months having improved predictions when bromine and
452 iodine chemistry is included. This is especially true at coastal AQS sites where the bromine and
453 iodine chemistry improves model performance for all months except March and April. Gantt et
454 al. (2017) compared model (using a 12-km horizontal grid resolution) predictions for August
455 2006 with observations from the 2006 ship-based TexAQS and coastal AQS sites and reported
456 that the model without bromine and iodine chemistry generally over-predicts O₃ while the
457 bromine and iodine chemistry improves the model performance. Model performance shown in
458 Figures 8 and 10 for August is consistent with results of Gantt et al. (2017).

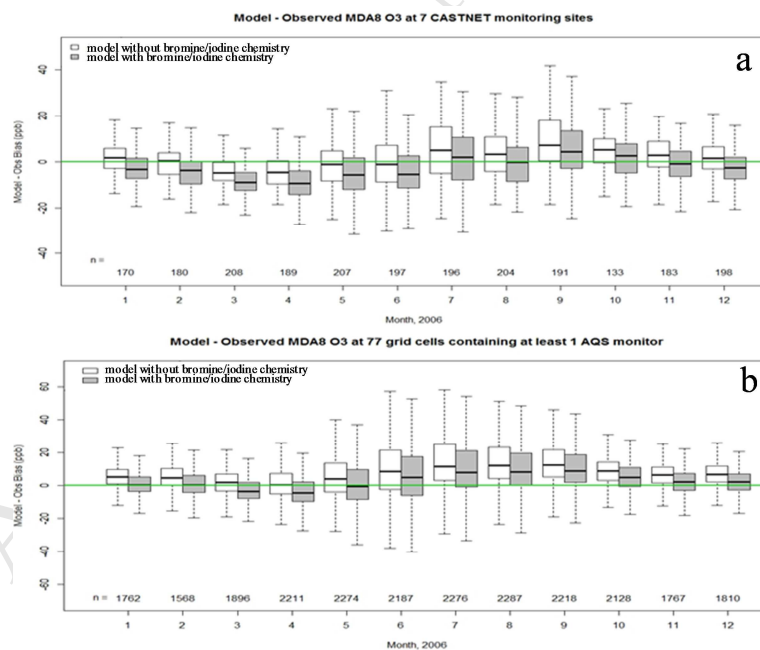
459



460

461 Figure 9. Monthly mean bias without (No_Br/I – Observations) and with (Added_Br/I – Observations) the bromine
 462 and iodine chemistry at all (a) CASTNET and (b) AQS sites. AQS observations falling within the same grid cell are
 463 first averaged prior to comparing to the model value. Lower bar in the box represents the 25th percentile, middle
 464 bar represents the median and the upper bar represents the 75 percentile values. The lowest horizontal bar represents the
 465 minimum value while the highest horizontal bar represents the maximum value.

466



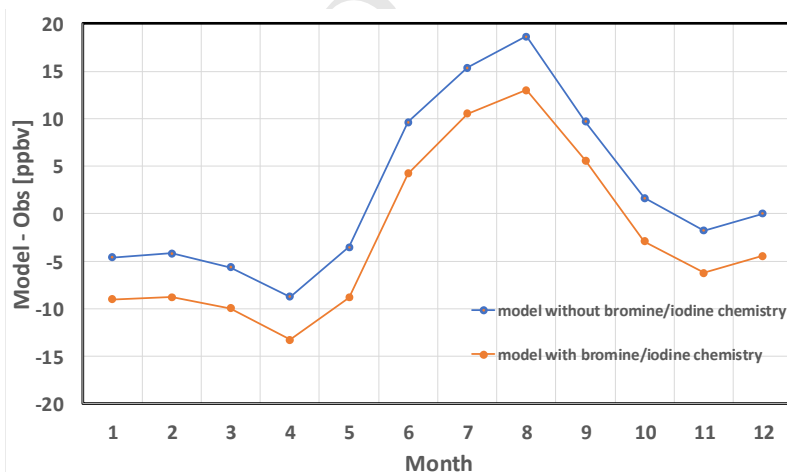
467

468 Figure 10. Monthly mean bias without (No_Br/I – Observations) and with (Added_Br/I – Observations) the bromine
 469 and iodine chemistry at coastal (a) CASTNET and (b) AQS sites. AQS observations falling within the same grid cell
 470 are first averaged prior to comparing to the model value. Lower bar in the box represents the 25th percentile, middle

471 bar represents the median and the upper bar represents the 75 percentile values. The lowest horizontal bar represents
 472 the minimum value while the highest horizontal bar represents the maximum value.
 473

474 The hemispheric domain also allows for model evaluation against O₃ observations from monitors
 475 in Japan as part of the Acid Deposition Monitoring Network in East Asia (www.eanet.asia/eanet)
 476 (Figure 11). The simulation without bromine and iodine chemistry underpredicts O₃ (by 2-9
 477 ppbv) during the cooler months (January-May and November) and overpredicts (by 2-19 ppbv)
 478 in the warmer months (June-September). Including bromine and iodine chemistry further
 479 deteriorates O₃ model performance in the cooler months but improves model performance in
 480 warmer months. This seasonality is consistent with Kyo et al. (2019) which reported CMAQ
 481 overpredictions of O₃ during the summertime over Japan.

482
 483
 484



485
 486 Figure 11. Monthly mean bias without (No_Br/I – Observations) and with (Added_Br/I – Observations) the bromine
 487 and iodine chemistry at monitoring sites in Japan.

488

489 4.0 SUMMARY

490 Regional chemical transport models like CMAQ are routinely applied to specific geographic
491 areas for developing air pollutant control strategies. Often the boundary conditions for the
492 regional models are adapted from hemispheric and global models to capture the broader
493 influence of global pollution on the focal region. The results of this study reveal that bromine
494 and iodine chemistry not only affects O₃ over seawater but also over land, improves model
495 performance for coastal sites, and reduces the predicted background ozone. These combined
496 impacts provide strong evidence that bromine and iodine chemistry should be considered for
497 inclusion in air quality models used for O₃ applications.

498

499 DISCLAIMER

500 The views expressed in this paper are those of the authors and do not necessarily represent the
501 views or policies of the U.S. EPA.

502 REFERENCES

- 503 1. Allan, B. J., McFiggans, G., Plane, J.M.C., 2000. Observations of iodine monoxide in the remote marine
504 boundary layer. *J. Geophys. Res.* 2000, 105, D11, 14,363-14369.
- 505 2. Appel, K.W.; Pouliot, G.; Simon, H.; Sarwar, G.; Pye, H.O.T.; Napelenok, S.; Akhtar, F.; Roselle, S.J., 2013.
506 Evaluation of dust and trace metal estimates from the Community Multiscale Air Quality (CMAQ) model version
507 5.0. *Geoscientific Model Development*, 2013, 6, 883-899.
- 508 3. Appel, K.W., Napelenok, S., Foley, K.M., Pye, H.O.T., Hogrefe, C., Luecken, D.J., Bash, J.O., Roselle, S.J.,
509 Pleim, J.E., Foroutan, H., Hutzell, W., Pouliot, G., Sarwar, G., Sarwar, G., Fahey, K., Gantt, B., Gilliam, R.C.,
510 Kang, D., Mathur, R., Schwede, D., Spero, T., Wong, D.C., Young, J., 2017. Overview and evaluation of the
511 Community Multiscale Air Quality (CMAQ) model version 5.1. *Geosci. Model Dev.* 2017, 10, 1703-1732.
- 512 4. Badia, A., Reeves, C. E. and Baker, A. R. and Saiz-Lopez, A. and Volkamer, R. and Koenig, T. K. and Apel, E.
513 C. and Hornbrook, R. S. and Carpenter, L. J. and Andrews, S. J. and Sherwen, T. and von Glasow, R. 2019.
514 Importance of reactive halogens in the tropical marine atmosphere: a regional modelling study using WRF-Chem.
515 *Atmos. Chem. Phys.*, 19, 3161-3189, <https://doi.org/10.5194/acp-19-3161-2019>.
- 516 5. Breton, M.L.; Bannan T.J.; Shallcross, D.E.; Khan, M.A.; Evans, M.J.; Lee, J.; Lidster, R.; Andrews, S.;
517 Carpenter, L. J.; Schmidt, J.; Jacob, D.; Harris, N.R.P.; Bauguutte, S.; Gallagher, M.; Bacak, A.; Leather, K.E.;
518 Percival, C.J., 2017. Enhanced ozone loss by active inorganic bromine chemistry in the tropical troposphere.
519 2017, 155, 21-28.
- 520 6. Cooper, O.R.; Parrish; D.D.; Stohl, A.; Trainer, M.; Nédélec, P.; Thouret, V.; Cammas, J.P.; Oltmans, S. J.;
521 Johnson, B. J.; Tarasick, D.; Leblanc, T.; McDermid, I.S.; Jaffe, D.; Gao, R.; Stith, J.; Ryerson, T.; Aikin, K.;
522 Campos, T.; Weinheimer, A.; Avery, M.A., 2010. Increasing springtime ozone mixing ratios in the free
523 troposphere over western North America. *Nature* 2010, 463, 344–348.
- 524 7. Czader, B. H., X. Li, and B. Rappenglueck, 2013. CMAQ modeling and analysis of radicals, radical precursors,
525 and chemical transformations. *J. Geophys. Res. Atmos.*, 118, 11,376–11,387, doi:10.1002/jgrd.50807.
- 526 8. Damian, V., Sandu, A., Damian, M., Potra, F., and G. R. Carmichael., 2002. The Kinetic PreProcessor KPP – A
527 software environment for solving chemical kinetics. *Computers and Chemical Engineering*, 2002, 26(11), 1567-
528 1579.
- 529 9. David, L. M, Nair, P. R. 2011. Diurnal and seasonal variability of surface ozone and NOx at a tropical coastal
530 site: Association with mesoscale and synoptic meteorological conditions, *J. Geophys. Research*, 116, D10303.
- 531 10. Dickerson, R. R., Rhoads, K. P., Carsey, T. P., Oltmans, S. J., Burrows, J. P., Crutzen, P. J., 1999. Ozone in the
532 remote marine boundary layer: A possible role for halogens. *Geophys. Res.*, 104, 21385-21395.
- 533 11. Dix, B., Baider, S., Bresch, J. F., Hall, S.R., Schmidt, K. S., Wang, S., Volkamer, R., 2013. Detection of iodine
534 monoxide in the tropical free troposphere. *PNAS*, 2013, 110, 6, 2035-2040.
- 535 12. Dolwick, P.; Akhtar, F.; Baker, K. R.; Possiel, N.; Simon, H.; Tonnesen, G., 2015. Comparison of background
536 ozone estimates over the western United States based on two separate model methodologies. *Atmos. Environ.*
537 2015, 109, 282–296.
- 538 13. Environmental Protection Agency. 2016. Implementation of the 2015 Primary Ozone NAAQS: Issues Associated
539 with Background Ozone White Paper for Discussion, accessed at
540 <https://www.epa.gov/sites/production/files/2016-03/documents/whitepaper-bgo3-final.pdf>.
- 541 14. Fahey, K.M., Carlton, A.G., Pye, H.O.T., Baek, J., Hutzell, W.T., Stanier, C.O., Baker, K.R., Appel, K.W., Jaoui,
542 M., and J.H. Offenberg., 2017. A framework for expanding aqueous chemistry in the Community Multiscale Air
543 Quality (CMAQ) model version 5.1. *Geosci. Model Dev.*, 2017, 10, 1587–1605.
- 544 15. Fernandez, R. P.; Salawitch, R. J.; Kinnison, D. E.; Lamarque, J.-F.; Saiz-Lopez, A., 2014. Bromine partitioning
545 in the tropical tropopause layer: implications for stratospheric injection. *Atmospheric Chemistry and Physics*,
546 2014, 14, 13391-13410.
- 547 16. Fiore, A.M., Jacob, D.L., Bey, I., Yantosca, R.M., Field, B.D., Fusco, A.C., Wilkinson, J.G., 2002. Background
548 ozone over the United States in summer: origin, trend, and contribution to pollution episodes. *J. Geophys. Res.*
549 107 (D15), 4275.
- 550 17. Fiore, A.M., Jacob, D.J., Liu, H., Yantosca, R.M., Fairlie, T.D., Li, Q., 2003. Variability in surface ozone
551 background over the United States: Implications for air quality policy. *J. Geophys. Res.* 108 (D24), 4787.
- 552 18. Fiore, A.M., Oberman, J.T., Lin, M., Zhang, L., Clifton, O.E., Jacob, D.J., Naik, V., Horowitz, L.W., Pinto, J.P.,
553 Milly, G.P., 2014. Estimating North American background ozone in U.S. surface air with two independent global
554 models: variability, uncertainties, and recommendations. *Atmos. Environ.* 96, 284-300.

- 555 19. Gantt, B.; Kelly, J. T.; and Bash, J. O., 2015. Updating sea spray aerosol emissions in the Community Multiscale
556 Air Quality (CMAQ) model version 5.0.2. *Geosci. Model Dev.*, 8, 3733–3746, doi:10.5194/gmd-8-3733-2015,
557 2015.
- 558 20. Gantt, B., Sarwar, G.; Xing, J.; Simon, H.; Schwede, D.; Hutzell, W.T.; Mathur, R.; Saiz-Lopez, A., 2017. The
559 impact of iodide-mediated ozone deposition and halogen chemistry on surface ozone concentrations across the
560 continental United States. *Environmental Science & Technology*, 2017, 51(3), 1458-1466.
- 561 21. Kyo, K, Morino, Y., Yamaji, K., Chatani, S., 2019. Uncertainties in O₃ concentrations simulated by CMAQ over
562 Japan using four chemical mechanisms. *Atmospheric Environment*, 2019, 198, 448-462.
- 563 22. Long, M. S.; Keene, W. C.; Easter, R.; Sander, R.; Kerkweg, A.; Erickson, D.; Liu, X.; Ghan, S., 2013.
564 Implementation of the chemistry module MECCA (v2.5) in the modal aerosol version of the Community
565 Atmosphere Model component (v3.6.33) of the Community Earth System Model. *Geosci. Model Dev.*, 6, 255-
566 262, <https://doi.org/10.5194/gmd-6-255-2013>, 2013.
- 567 23. Long, M. S.; Keene, W. C.; Easter, R. C.; Sander, R.; Liu, X.; Kerkweg, A.; Erickson, D., 2014. Sensitivity of
568 tropospheric chemical composition to halogen-radical chemistry using a fully coupled size-resolved multiphase
569 chemistry–global climate system: halogen distributions, aerosol composition, and sensitivity of climate-relevant
570 gases. *Atmos. Chem. Phys.*, 2014, 14, 3397-3425
- 571 24. Mahajan, A. S., Plane, J. M. C., Oetjen, H., Mendes, L., Saunders, R. W., Saiz-Lopez, A., Jones, C. E., Carpenter,
572 L. J., and McFiggans, G. B., 2010. Measurement and modelling of tropospheric reactive halogen species over the
573 tropical Atlantic Ocean. *Atmos. Chem. Phys.*, 2010, 10, 4611-4624.
- 574 25. Mathur, R.; Xing, J., Gilliam, R.; Sarwar, G.; Hogrefe, C.; Pleim, J.; Pouliot, G.; Roselle, S.; Spero, T.; Wong,
575 D.C.; Young, J., 2017. Extending the Community Multiscale Air Quality (CMAQ) Modeling System to
576 Hemispheric Scales: Process Considerations and Initial Applications, *Atmos. Chem. Phys.*, 2017, 17, 1-25.
- 577 26. McDonald S. M.; Martin, J.C.G.; Chance, R., Warriner, S.; Saiz-Lopez, A.; Carpenter, LJ, Plane JMC., 2014. A
578 laboratory characterisation of inorganic iodine emissions from the sea surface: dependence on oceanic variables
579 and parameterisation for global modelling. *Atmospheric Chemistry & Physics*, 2014, 14, 5841-5852.
- 580 27. McDonald-Buller, E. C.; Allen, D. T.; Brown, N.; Jacob, D. J.; Jaffe, D. A.; Kolb, C. E.; Lefohn, A. S.; Oltmans,
581 S.; Parrish, D. D.; Yarwood, G.; Zhang, L. 2011. Establishing policy relevant background (PRB) ozone
582 concentrations in the United States. *Environ. Sci. Technol.* 2011, 45 (22), 9484–9497.
- 583 28. McFiggans, G.; Plane, JMC; Allan, BJ, Carpenter, LJ; Coe, H; O'Dowd, C., 2000. A modeling study of iodine
584 chemistry in the marine boundary layer. *Journal of Geophysical Research*, 2000, 105, D11, 14,371-14,385
- 585 29. Millero, F. J., 1996. *Chemical Oceanography*, second ed. CRC Press, Boca Raton, FL.
- 586 30. Muñoz-Unamunzaga, M.; Borge, B.; Sarwar, G.; Gantt, B.; Paz, D. P., Cuevas, C.A.; Saiz-Lopez, A., 2018. Ocean
587 halogen and sulfur emissions influence air quality in the coastal megacity of Los Angeles. *Science of the Total*
588 *Environment*, 2018, 610-611, 1536-1545.
- 589 31. Ordóñez, C.; Lamarque, J.-F.; Tilmes, S.; Kinnison, D. E.; Atlas, E. L.; Blake, D. R.; Sousa Santos, G.; Brasseur,
590 G.; Saiz-Lopez, A., 2012. Bromine and iodine chemistry in a global chemistry-climate model: description and
591 evaluation of very short-lived oceanic sources. *Atmospheric Chemistry & Physics*, 2012, 12, 1423-1447.
- 592 32. Otte, T.L.; Pleim, J.E., 2010. The Meteorology-Chemistry Interface Processor (MCIP) for the CMAQ modeling
593 system: updates through MCIPv3.4.1. *Geosci. Model Dev.*, 2010, 3, 243–256.
- 594 33. Parrella, J. P.; Jacob, D. J.; Liang, Q.; Zhang, Y.; Mickley, L. J.; Miller, B.; Evans, M. J.; Yang, X.; Pyle, J. A.;
595 Theys, N.; Van Roozendaal, M., 2012. Tropospheric bromine chemistry: implications for present and pre-
596 industrial ozone and mercury. *Atmospheric Chemistry & Physics*, 2012, 12, 6723–6740.
- 597 34. Parrish, D. D.; Millet, D. B.; Goldstein, A. H., 2009. Increasing ozone in marine boundary layer air inflow at the
598 west coasts of North America and Europe. *Atmos. Chem. Phys.* 2009a, 9, 1303–1323.
- 599 35. Parrish, D. D.; Allen, D. T.; Bates, T. S.; Estes, M.; Fehsenfeld, F. C.; Feingold, G.; Ferrare, R.; Hardesty, R. M.;
600 Meagher, J. F.; Nielsen-Gammon, J. W.; Pierce, R. B.; Ryerson, T. B.; Seinfeld, J. H.; Williams, E. J., 2009.
601 Overview of the Second Texas Air Quality Study (TexAQS II) and the Gulf of Mexico Atmospheric Composition
602 and Climate Study (GoMACCS). *J. Geophys. Res.* 2009b, 114.
- 603 36. Peters, C., Pechtl, S., Stutz, J., Hebestreit, K., Hönninger, G., Heumann, K. G., Schwarz, A., Winterlik, J., Platt,
604 U., 2005. Reactive and organic halogen species in three different European coastal environments. *Atmos. Chem.*
605 *Phys.*, 5, 3357-3375, 2005.
- 606 37. Qiao, X.; Ying, Q.; Li, X.; Zhang, H.; Hu, J.; Tang, Y.; Chen, X., 2018. Source apportionment of PM_{2.5} for 25
607 Chinese provincial capitals and municipalities using a source-oriented Community Multiscale Air Quality model.
608 *Atmospheric Environment*, 2018, 612, 462-471, 2018.
- 609 38. Read, K. A.; Mahajan, A. S.; Carpenter, L. J.; Evans, M. J.; Faria, B. V. E.; Heard, D. E.; Hopkins, J. R.; Lee, J.
610 D.; Moller, S. J.; Lewis, A. C.; Mendes, L.; McQuaid, J. B.; Oetjen, H.; Saiz-Lopez, A.; Pilling, M. J.; Plane, J.

- 611 M. C., 2008. Extensive halogen mediated ozone destruction over the tropical Atlantic Ocean. *Nature*, 2008, 453,
612 1232–1235
- 613 39. Ring, A.M.; Canty, T.P.; Anderson, D.C.; Vinciguerra, T.P.; e, H; Goldberg, D.L.; Ehrman, S.H.; Dickerson,
614 R.R.; Salawitch, R.J., 2018. Evaluating commercial marine emissions and their role in air quality policy using
615 observations and the CMAQ model. *Atmospheric Environment*, 173, 96–107, 2018.
- 616 40. Sarwar, G.; Simon, H.; Bhawe, P; G. Yarwood, G., 2012. Examining the impact of heterogeneous nitryl chloride
617 production on air quality across the United States. *Atmospheric Chemistry and Physics*, 2012, 12, 1–19.
- 618 41. Sarwar, G., Gantt, B.; Schwede, D.; Foley, K.; Mathur, R.; Saiz-Lopez, A., 2015. Impact of enhanced ozone
619 deposition and halogen chemistry on tropospheric ozone over the Northern Hemisphere, *Environmental Science
620 & Technology*, 2015, 49(15):9203–9211.
- 621 42. Saiz-Lopez, A., Shillito, J.A., Coe, H., Plane, J. M. C., 2006. Measurements and modelling of I₂, IO, OIO, BrO,
622 and NO₃ in the mid-latitude marine boundary layer. *Atmos. Chem. Phys.*, 6, 1513–1528, 2006.
- 623 43. Saiz-Lopez, A., Mahajan, A. S., Salmon, R. A., Bauguitte, S. J.-B., Jones, A. E., Roscoe, H. K. Plane, J. M. C.,
624 2007. Boundary Layer Halogens in Coastal Antarctica, *Science* (80-.), 317(5836), 348–351,
625 doi:10.1126/science.1141408, 2007.
- 626 44. Saiz-Lopez, A., Lamarque, J.-F., Kinnison, D. E., Tilmes, S., Ordóñez, C., Orlando, J. J., Conley, A. J., Plane, J.
627 M. C., Mahajan, A. S., Sousa Santos, G., Atlas, E. L., Blake, D. R., Sander, S. P., Schauffler, S., Thompson, A.
628 M. and Brasseur, G., 2012. Estimating the climate significance of halogen-driven ozone loss in the tropical
629 marine troposphere. *Atmos. Chem. Phys.*, 12(9), 3939–3949, doi:10.5194/acp-12-3939-2012, 2012.
- 630 45. Saiz-Lopez, A.; Fernandez, R. P.; Ordóñez, C.; Kinnison, D. E.; Gómez Martín, J. C.; Lamarque, J.-F.; Tilmes,
631 S., 2014. Iodine chemistry in the troposphere and its effect on ozone. *Atmos. Chem. Phys.*, 2014, 14, 13119–
632 13143.
- 633 46. Schmidt, J. A.; Jacob, D. J.; Horowitz, H. M.; Hu, L.; Sherwen, T.; Evans, M. J.; Liang, Q.; Suleiman, R. M.;
634 Oram, D. E.; Breton, M. L.; Percival, C. J.; Wang, S.; Dix, B.; and Volkamer, R. 2016. Modeling the observed
635 tropospheric BrO background: importance of multiphase chemistry and implications for ozone, OH, and mercury,
636 *J. Geophys. Res.-Atmos.*, 2016, 121, 11819–11835.
- 637 47. Sherwen, T., Evans, M. J., Carpenter, L. J., Andrews, S. J., Lidster, R. T., Dix, B., Koenig, T. K., Sinreich, R.,
638 Ortega, I., Volkamer, R., Saiz-Lopez, A., Prados-Roman, C., Mahajan, A. S., and Ordóñez, C., 2016. Iodine's
639 impact on tropospheric oxidants: a global model study in GEOS-Chem. *Atmos. Chem. Phys.*, 2016a, 16, 1161–
640 1186.
- 641 48. Sherwen, T., Schmidt, J. A., Evans, M. J., Carpenter, L. J., Großmann, K., Eastham, S. D., Jacob, D. J., Dix, B.,
642 Koenig, T. K., Sinreich, R., Ortega, I., Volkamer, R., Saiz-Lopez, A., Prados-Roman, C., Mahajan, A. S.,
643 Ordóñez, C., 2016. Global impacts of tropospheric halogens (Cl, Br, I) on oxidants and composition in GEOS-
644 Chem. *Atmos. Chem. Phys.*, 2016b, 16, 12239–12271.
- 645 49. Skamarock, W. C.; Klemp, J.B.; Dudhia, J.; Grill, D.O.; Barker, D.M.; Duda, M.G.; Huang, X-Y; Wang, W.
646 Powers, J.G. A description of the advanced research WRF version 3. NCAR Tech Note NCAR/TN 475 STR,
647 2008, 125 pp. [Available from UCAR Communications, P.O. Box 3000, Boulder, CO 80307.]
- 648 50. von Glasow, R.; Sander, R.; Bott, A.; Crutzen, P.J. 2002. Modeling of halogen chemistry in the marine boundary
649 layer. 1. Cloud-free MBL. *J. Geophysical Research*, 2002, 107, 4341.
- 650 51. von Glasow, R.; Sander, R.; Bott, A.; Crutzen, P. J. 2002. Modeling halogen chemistry in the marine boundary
651 layer. 2. Interactions with sulfur and cloud-covered MBL. *J. Geophys. Res.* 2002, 107, 4323.
- 652 52. Wang, S.; Schmidt, J.A., Baidar, S., Coburn, S., Dix, B., Koenig, T. K., Apel, E., Bowdalo, D., Campos, T.L.,
653 Eloranta, E., Evans, M. J., DiGangi, J.P., Zondlo, M.A., Gao, R., Haggerty, J.A., Hall, S. R., Hornbrook, R.S.,
654 Jacob, D., Morley, B., Pierce, B., Reeves, M., Romashkin, P., Schure A., and Volkamer, R., 2015. Active and
655 widespread halogen chemistry in the tropical and subtropical free troposphere, *PNAS*, 2015, 112 (30) 9281–9286
- 656 53. Yang, X.; Cox, R. A.; Warwick, N. J.; Pyle, J. A.; Carver, G. D.; O'Connor, F. M.; Savage, N. H., 2005.
657 Tropospheric bromine chemistry and its impacts on ozone: A model study. *Journal of Geophysical Research*,
658 2005, 110, D23311.
- 659 54. Yarwood, G.; Jung, J.; Whitten, G. Z.; Heo, G.; Mellberg, J.; Estes, M., 2010. UPDATES TO THE CARBON
660 BOND MECHANISM FOR VERSION 6 (CB6), Presented at the 9th Annual CMAS Conference, Chapel Hill,
661 NC, October 11–13, 2010. Available at
662 https://www.cmascenter.org/conference/2010/abstracts/emery_updates_carbon_2010.pdf
- 663 55. Yu, S., R. Mathur, G. Sarwar, D. Kang, D. Tong, G. Pouliot, J. Pleim, 2010. Eta-CMAQ air quality forecasts for
664 O₃ and related species using three different photochemical mechanisms (CB4, CB05, SAPRC-99): comparisons
665 with measurements during the 2004 ICARTT study, *Atmospheric Chemistry & Physics*, 10, 3001–3025.

- 666 56. Zhang, L.; Jacob, D. J.; Downey, N. V.; Wood, D. A.; Blewitt, D.; Carouge, C. C.; van Donkelaar, A.; Jones, D.
667 B. A.; Murray, L. T.; Wang, Y., 2011. Improved estimate of the policy-relevant background ozone in the United
668 States using the GEOS-Chem global model with $1/2^\circ \times 2/3^\circ$ horizontal resolution over North America. *Atmos.*
669 *Environ.* 2011, 45 (37), 6769–6776.
670
671

ACCEPTED MANUSCRIPT

Highlights

- Bromine and iodine chemistry reduces ozone
- Iodine chemistry is more effective in reducing ozone than the bromine chemistry
- Bromine and iodine chemistry affects background ozone
- Bromine and iodine chemistry improves model performance

Declaration of interests

The authors declare that they have no known competing financial interests or personal relationships that could have appeared to influence the work reported in this paper.

The authors declare the following financial interests/personal relationships which may be considered as potential competing interests: